Ground state, phonon spectrum, and superconducting properties of the nonoxide perovskite $CdCNi_3$

S. Bağcı,[1] S. Duman,[1] H. M. Tütüncü,[1] and G. P. Srivastava[2]
[1]*Sakarya Üniversitesi, Fen-Edebiyat Fakültesi, Fizik Bölümü, 54187, Adapazarı, Turkey*
[2]*School of Physics, University of Exeter, Stocker Road, Exeter EX4 4QL, United Kingdom*
(Received 20 June 2008; revised manuscript received 29 August 2008; published 6 November 2008)

We have made theoretical investigations of the structural, elastic, electronic, lattice-dynamical, and superconducting properties of the antiperovskite compound $CdCNi_3$. The structural, elastic, and electronic properties of this material have been calculated by using the generalized gradient approximation of the density-functional theory and *ab initio* pseudopotentials. Using our structural and electronic results, the phonon spectrum, phonon linewidths, and electron-phonon coupling parameter have been calculated by employing a linear-response approach based on density-functional theory. We have observed a softening behavior of the lowest acoustic phonon branch along the *X*-*R* symmetry direction. The electron-phonon coupling parameter is found to be 0.80.

DOI: 10.1103/PhysRevB.78.174504 PACS number(s): 74.25.Kc, 74.25.Jb, 71.15.Mb, 63.20.dk

I. INTRODUCTION

The discovery of superconductivity in $MgCNi_3$, with the superconducting transition temperature [T_C=8 K (Ref. 1)], has been quite unexpected. This is because with the partially filled Ni *d* orbitals $MgCNi_3$ is expected to possess a ferromagnetic ground state rather than superconducting state. This led Rosner *et al.*[2] to suggest that magnetic interactions may support superconductivity in this material. However, experimental measurements[3–6] indicate that $MgCNi_3$ is an *s*-wave BCS superconductor. On the theoretical side, there have been a number of first-principles electronic structure calculations using the tight-binding linear muffin-tin orbital (TB-LMTO) method,[7] the linear muffin-tin orbital (LMTO) method,[4,8] full-potential nonorthogonal local-orbital (FPLO) minimum-basis scheme,[9] and the appropriate band-structure method (like ultrasoft pseudopotential method)[10–13] to understand the electronic properties of $MgCNi_3$. All these studies have observed a sharp peak just below the Fermi level in the electronic density of states for $MgCNi_3$. It is well known that the high-electronic density of states at the Fermi level is favorable to superconductivity. In addition to electronic properties, the lattice dynamics of this material has been investigated using density-functional theory within LMTO,[14] *ab initio* mixed-basis perturbation method,[15] and the appropriate band-structure method (like ultrasoft pseudopotential method).[13] All of these studies have found anomalous behavior in the lowest acoustic-phonon branch along each of the high-symmetry directions [100], [110], and [111]. These phonon calculations also indicated that the largest contribution to the electron-phonon mass enhancement parameter (i.e., average electron-phonon coupling parameter) comes from phonon branches which show anomalous dispersion. For example, the average electron-phonon coupling parameter was found to be 1.51 in the LMTO work by Ignatov *et al.*[14] Thus the existing theoretical works have confirmed the experimental works that $MgCNi_3$ is a BCS-type superconductor with large electron-phonon interaction.

The successful explanation of the BCS-type superconductivity in $MgCNi_3$ has led to the research in the superconducting property of other nickel-based antiperovskites $ACNi_3$ (A=Cd, Zn, Al, and Ga).[12,16–25] In particular, superconducting properties of $CdCNi_3$ was reported in the experimental work by Uehara *et al.*[23] In their work, they have indicated that this material is a newly synthesized superconductor with T_C=2.5–3.2 K. Following this experimental work, full-potential linearized augmented plane-wave method with the generalized gradient approximation has been used to calculate structural, elastic, and electronic properties of $CdCNi_3$.[24,25] This theoretical calculation clearly showed that there is a sharp peak below the Fermi level in the electronic density of states in this material. As we have mentioned before, this feature is very important for superconductivity. In contrast to the structural, elastic, and electronic properties of $CdCNi_3$, there are no reports of its vibrational properties. An accurate description of vibrational properties of this material is important, both from lattice dynamics viewpoint as well as for determining the electron-phonon interaction parameter needed to understand superconductivity.

The aim of the present paper is to investigate the structural, elastic, and electronic properties of $CdCNi_3$ by employing an *ab initio* pseudopotential method based on the density-functional theory within the generalized gradient approximation. A linear-response scheme based on the above method is employed to calculate phonon-dispersion relations. Using these results, we discuss the role of phonon softening on superconductivity by calculating the electron-phonon interaction parameter.

II. THEORY

We use the first-principles pseudopotential method based on the density-functional theory. The electron-ion interaction was described by using ultrasoft pseudopotentials.[26] The density-functional theory has been implemented within the generalized gradient approximation, using the Perdew-Burke-Ernzerhof method.[27] A basis set containing all plane waves up to the cut-off energy of 60 Ry has been used. For structural, elastic, and electronic properties, Brillouin-zone integrations were performed using the $24\times24\times24$ Monkhorst-Pack **k**-point mesh.[28]

TABLE I. Structural and elastic properties of $CdCNi_3$ and their comparison with previous theoretical results.

Source	a (Å)	B (Mbar)	B'	C_{11} (Mbar)	C_{12} (Mbar)	C_{44} (Mbar)
This work	3.863	1.773	4.510	3.190	1.064	0.601
Experimental (Ref. 23)	3.844					
Theory (Ref. 24)	3.867	1.8831		3.115	1.267	0.572

A cubic crystal has three independent elastic constants: C_{11}, C_{12}, and C_{44}. The straightforward manner of obtaining these constants is to calculate the total-energy difference between an unstrained medium and a distorted medium at constant volume. We have used the volume-conserving tetragonal and monoclinic strains for C_{11}-C_{12} and C_{44}, respectively.[29,30] In order to obtain C_{11} and C_{12} separately, the relationship between these elastic constants and bulk modulus

$$B = \frac{1}{3}(C_{11} + 2C_{12}) \tag{1}$$

is also used.

The lattice dynamics of $CdCNi_3$ was studied in the framework of the harmonic approximation to the force constants and using the linear-response method[31,32] which is realized in the QUANTUM ESPRESSO code.[32] Within this scheme, second-order derivatives of the total energy were calculated to obtain the dynamical matrix. A static linear response of the valence electrons was considered in terms of the variation of the external potential corresponding to periodic displacements of the atoms in the unit cell. The screening of the electronic system in response to the displacement of the atoms was taken into account in a self-consistent manner. Integration up to the Fermi surface is done by employing the smearing technique with the broadening parameter σ=0.02 Ry. For the Brillouin-zone integration we use the $16\times16\times16$ Monkhorst-Pack **k** mesh in the irreducible Brillouin zone. The dynamical matrices have been computed on a $4\times4\times4$ **q**-point mesh and a Fourier interpolation has been used to calculate phonons for any chosen **q** point. The technique for the calculation of the electron-phonon coupling has been described in detail in our previous work.[13] Fermi-surface sampling for the evaluation of the electron-phonon matrix elements was done using $28\times28\times28$ **k** mesh with the Gaussian width σ=0.02 Ry. The phonon density of states and the Eliashberg function were also calculated for this mesh. In order to check the appropriateness of our choice for the smearing parameter (σ=0.02 Ry), we have calculated the total density of states at the Fermi level [$N(E_F)$] against different values of smearing parameter around our choice. The value of $N(E_F)$ is found to be 3.83 states/eV for σ=0.01 Ry, 3.83 states/eV for σ=0.015 Ry, 3.82 states/eV for σ=0.02 Ry, 3.82 states/eV for σ=0.025 Ry, and 3.81 states/eV for σ=0.03 Ry. As can be seen from these results, our choice for the smearing parameter is acceptable.

III. RESULTS

A. Structural and elastic properties

$CdCNi_3$ crystallizes in the cubic antiperovskite structure with the space-group symmetry $Pm\bar{3}m$ where the atomic positions are: Cd at (0,0,0), C at (0.5,0.5,0.5), and Ni at (0.5,0.5,0), (0.5,0,0.5), and (0, 0.5, 0.5). In this structure, there are six Ni atoms at the face-centered positions of each unit cell forming a three-dimensional network of Ni_6 octahedron similar to oxygen octahedron in $CaTiO_3$. Each C atom is located in the body-centered cubic position surrounded by the Ni_6-octahedron cage. This is usually referred to as the cubic antiperovskite structure due to Ni atoms occupying anion positions in the $CaTiO_3$ perovskite structure.[33] In order to obtain the structural properties of $CdCNi_3$, the total energies are calculated for different volumes around the equilibrium volume V_0. The calculated total energies are fitted to the Murnaghan's equation of state[34] to determine the structural properties such as the equilibrium lattice constant (a), the bulk modulus (B), and its pressure derivative (B'). The calculated values of these parameters are presented and compared with previous experimental[23] and theoretical[24] works in Table I. The calculated lattice constant is overestimated by 0.5% compared to its experimental value.[23] This level of disagreement is quite common for theories based on the generalized gradient approximation. To the best of our knowledge, there are no experimental data for bulk modulus and its pressure derivative for us to compare. On the other hand, the difference between ours and previous theoretical calculations[24] is around 6%.

In Table I, we also show our computed elastic constants for $CdCNi_3$ at zero pressure. For cubic crystals, the mechanical stability requires the elastic constants to satisfy the well-known Born stability criteria[35]

$$C_{44} > 0, \quad C_{11} - C_{12} > 0, \quad C_{11} + 2C_{12} > 0.$$

Our results clearly suggest that the cubic $CdCNi_3$ is mechanically stable. Unfortunately, we have not been able to find any experimental data for the elastic constants of this material to compare our results. For comparison, we have presented previous theoretical results from Ref. 24 in this table: We identify that the deviations range between 2% and 16%, the worst agreement being found for C_{12}.

B. Electronic properties

The calculated energy-band structure, at the equilibrium lattice constant for $CdCNi_3$, along the high-symmetry directions in the simple-cubic Brillouin zone (BZ) is shown in

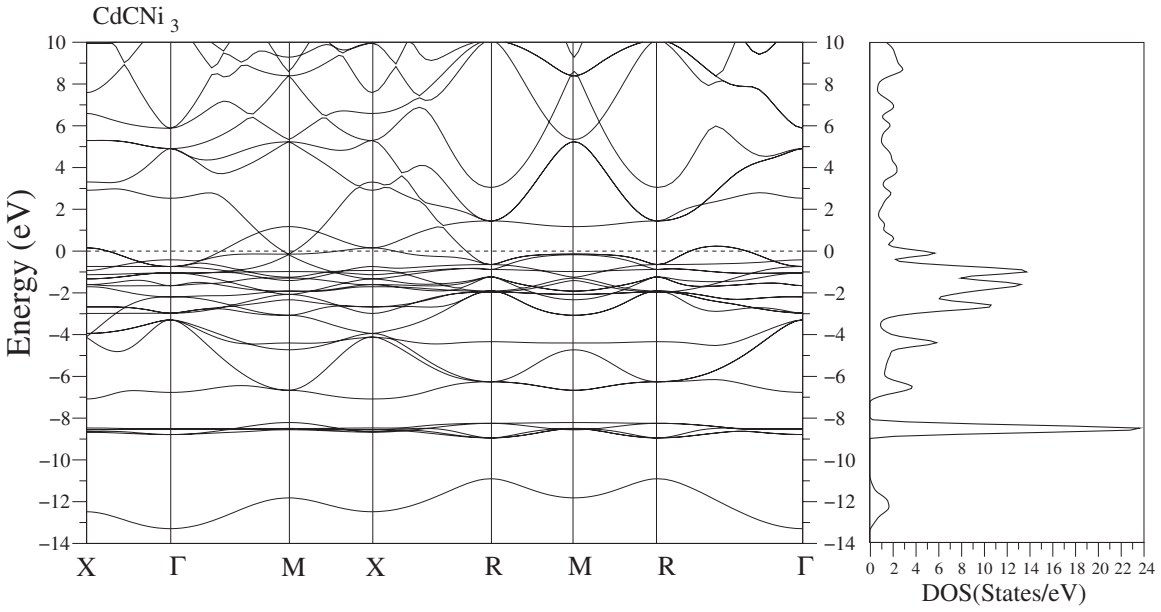

FIG. 1. The electronic band structure and DOS for $CdCNi_3$. The Fermi level corresponds to 0 eV.

Fig. 1. The valence and conduction bands considerably overlap along the Γ-*M* and *M*-*X* symmetry lines, confirming the metallicity of this material. The overall band profiles are found to be in fairly good agreement with previous theoretical results.[24,25] Figure 1 also illustrates the total density of states (DOS). The DOS has peaks at −12.3, −8.6, and −6.6 and a cluster of peaks between −5 eV and the Fermi level. The peak at −12.3 eV is characterized by C 2*s* states. The peak at −8.6 eV is mainly dominated by Cd 4*d* states, with small contributions from Ni 4*s* and 3*d* states. The peak at −6.6 eV is mixed with contributions from C 2*p*, Cd 5*s*, and Ni 4*s*+3*d* states.

In the energy range from −5 to 0 eV, there are five peaks with energies −4.5, −2.7, −1.6, −1.1, and −0.14 eV. These are mainly dominated by 3*d* electrons of Ni atom but with small C and Cd *p* contributions. It is interesting to note that in a previous work we also observed five peaks in the total DOS of $MgCNi_3$ in this energy range.[13] In particular, there is a peak at around 0.1 eV below the Fermi level for both materials. This peak is very important for governing superconducting properties of both these materials, as Cooper pairs in the BCS theory can be formed by electrons which have energies close to the Fermi level.

The DOS at the Fermi level $[N(E_F)]$ is found to be 3.82 states/eV in our calculations. The contribution of Ni 3*d* states to the $N(E_F)$ is as much as 80%. A similar observation was previously made for the electronic properties of $MgCNi_3$. A small amount of C and Cd *p* states is mixed with Ni 3*d* states. From $N(E_F)$, the electronic specific-heat coefficient is calculated using the expression

$$\frac{C_{\mathrm{el}}}{T} \sim \frac{\pi^2}{3} k_B N(E_F). \tag{2}$$

From our work this comes around 9.01 $\mathrm{mJ/mol\ K^2}$. This value can be compared with 10.58 $\frac{\mathrm{mJ}}{\mathrm{mol\ K^2}}$ in the theoretical work by Shein *et al.*[24] The measured specific-heat coefficient was reported to be 18.0 $\mathrm{mJ/mol\ K^2}$ by Uehara *et al.*[23] From the experimental and theoretical values of the specific heat $C_{\mathrm{el}}^{\mathrm{exp}}$ and $C_{\mathrm{el}}^{\mathrm{the}}$, respectively, the electron-phonon coupling parameter λ can be estimated using the following expression:[12,24,25,36]

$$C_{\mathrm{el}}^{\mathrm{exp}} = C_{\mathrm{el}}^{\mathrm{the}}(1+\lambda). \tag{3}$$

Using this expression, the estimated value of λ is found to be 0.99. This value will be compared with our directly calculated value in Sec. III C.

C. Phonons and superconductivity

After discussing the electronic properties of $CdCNi_3$, we turn our attention to its lattice-dynamical properties. In Fig. 2, the calculated phonon-dispersion relations are shown along several high-symmetry lines in the BZ together with the corresponding phonon density of states. Since the unit cell contains five atoms, there are 15 vibrational phonon modes for any chosen **q** point. However, transverse branches are degenerate along certain high-symmetry directions. Several features can be observed in this phonon spectrum. Due to the large mass difference between C and the heavier atoms Cd and Ni, the spectrum divides into two separate parts. In the frequency range from 15 to 19 THz, there are three high-frequency optical-phonon branches which are well separated from other modes distributed in the frequency range from 0 to 9 THz. Another interesting aspect of the phonon spectrum is the anomalous dispersion exhibited by the lowest acoustic branch along the *X*-*R* direction. This phonon branch exhibits a dip at $\mathbf{q}=\frac{2\pi}{a}(0.25,0.25,0.50)$, which is indicated by an arrow in Fig. 2. A similar behavior was also found in the phonon spectrum of $MgCNi_3$.[13] However, different from $MgCNi_3$,[13] no unstable phonon modes appear for $CdCNi_3$, indicating that the latter material is dynamically stable.

We speculate that there are two possible contributing factors to produce instability in the phonon spectrum of the

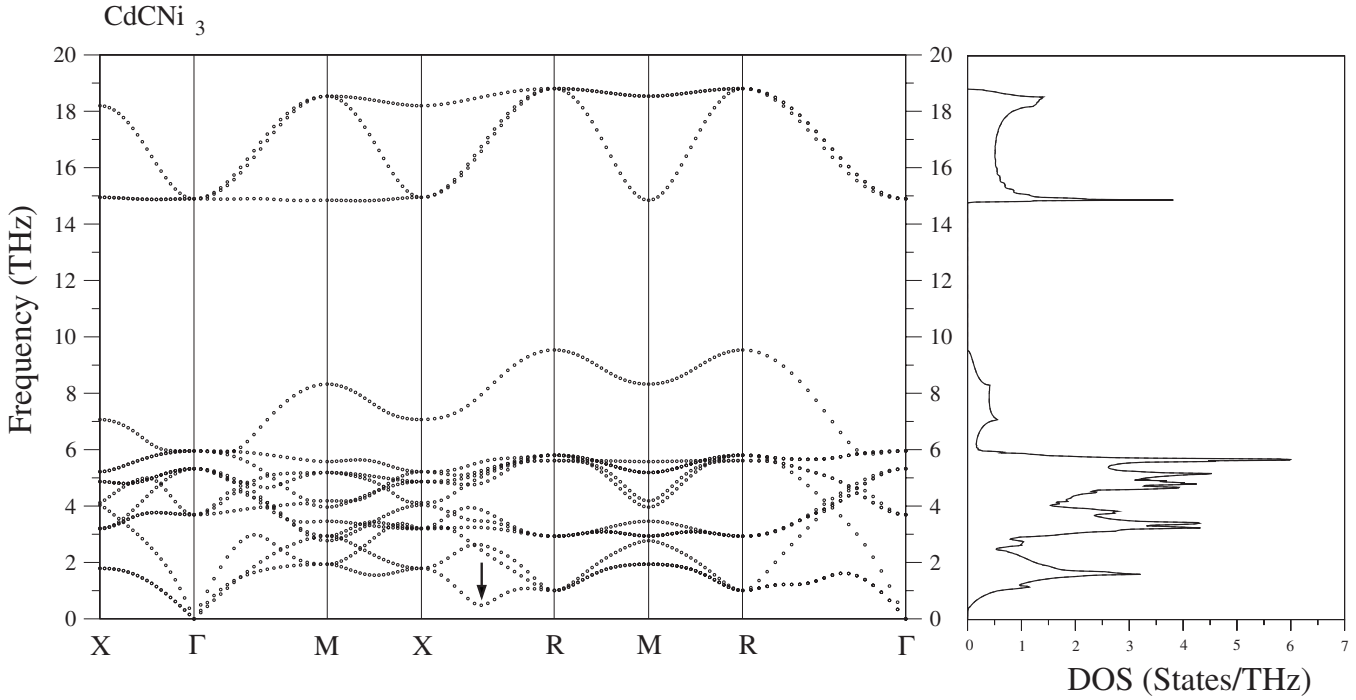

FIG. 2. Theoretical phonon-dispersion curves and density of states for $CdCNi_3$. The arrow indicates the anomalous phonon softening.

$ABNi_3$ class of materials: either an increase in the number of valence electrons in atom B or a change in the mass of atom A. Our previous work[13] suggests that an increase in the number of valence electrons in atom B produces instability. There is clearly no change in the number of valence electrons between $MgCNi_3$ and $CdCNi_3$ and the two materials have similar electronic properties. However, there is a big difference in the masses of Mg and Cd atoms. The lowest acoustic branch for $MgCNi_3$ is totally localized on the Ni atoms.[13] In contrast, in $CdCNi_3$ this branch also includes atomic vibrations from Cd due to the heavy mass of this atom. Thus, the overlap between Ni *d* orbitals in $CdCNi_3$ is weak, leading to the anomalous dispersion (but no instability) of this branch.

The calculated phonon density of states shows two continuum regions between 0 and 9 THz and between 15 and 19 THz. The upper continuum region is contributed by vibrations of the C and Ni atoms and shows two clear peaks at frequencies 14.9 and 18.2 THz. The three optical-phonon branches that encompass this region are split along the symmetry direction *M*-*X*. The lowest and highest of these branches are nearly flat while the intermediate one shows a large amount of dispersion with wave vector **q**. For the intermediate branch the eigen displacement of the heavy Ni atom increases from *M* to *X* and consequently leads to a downward dispersion. Below the gap region, there are four sharp peaks at frequencies 1.7, 3.3, 5.0, and 5.6 THz. These peaks are mainly characterized by the vibrations of Cd and Ni atoms due to a large mass difference between Cd (or Ni) and C atoms.

The zone-center phonon modes are of special interest in the lattice dynamics of solids. The optical-phonon modes in $CdCNi_3$ at the zone-center Γ point can be classified as

$$\Gamma = F_{1u}^1 + F_{1u}^2 + F_{1u}^3 + F_{2u}.$$

All these phonon modes are triply degenerate. None of these phonon modes is Raman active because in a perfect cubic structure all lattice sites have inversion symmetry. On the other hand, these phonon modes can be measured by infrared and neutron spectroscopies. In Table II, we have presented a comparison of zone-center phonon modes for $CdCNi_3$ and $MgCNi_3$.[13] Before comparing the results for these materials, it should be noted that the calculated lattice constants of these materials differ from each other by approximately 3%. As can be seen from Table II, the frequencies of the F_{2u} phonon modes for these materials are very close to each other because this phonon mode originates from the vibrations of Ni atoms. The 4% difference between the frequencies of this phonon mode can be related to the lattice-constant difference between these materials. The frequency difference between the F_{1u}^1 phonon mode of these materials is larger since this phonon mode includes large atomic vibrations from Cd atoms for $CdCNi_3$ and Mg atoms for $MgCNi_3$. Different from $MgCNi_3$, the F_{1u}^2 mode in $CdCNi_3$ includes large atomic vibrations from Ni atoms and some contribution from Cd atoms. As a result, 3 THz difference has been observed between the F_{1u}^2 mode of these materials. Finally, the

TABLE II. A comparison of zone-center phonon modes (in terahertz) of $CdCNi_3$ and $MgCNi_3$.

Material	F_{1u}^1	F_{1u}^2	F_{1u}^3	F_{2u}
$CdCNi_3$	3.69	5.96	14.89	5.32
$MgCNi_3$ (Ref. 13)	4.23	8.95	18.60	5.53

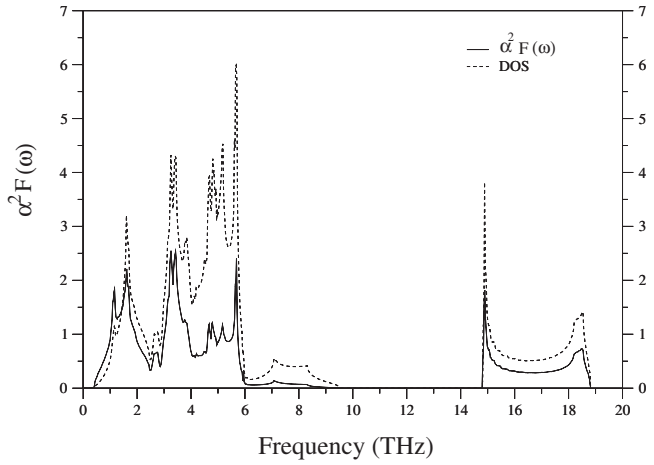

FIG. 3. A comparison of the phonon density of states (dashed lines) and Eliashberg spectral function $\alpha^2F(\omega)$ (solid lines).

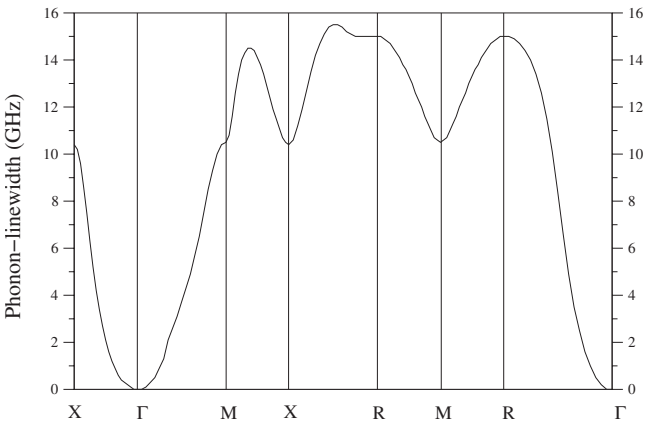

FIG. 4. Phonon linewidth of the lowest acoustic-phonon mode due to electron-phonon coupling along several high-symmetry directions in $CdCNi_3$.

highest optical frequency for $CdCNi_3$ differs by 20% from the corresponding phonon mode for $MgCNi_3$ due to a larger mass of Cd than Mg and slightly bigger lattice constant of $CdCNi_3$.

As we have mentioned before, the most interesting aspect of the dispersion curves of $CdCNi_3$ is the anomalous dispersion exhibited by the lowest acoustic branch along the *X*-*R* symmetry direction. This observation has motivated us to calculate electron-phonon coupling parameter along this symmetry direction. The lowest acoustic-phonon branch has a dip with the value of 0.55 THz at the $\mathbf{q}=\frac{2\pi}{a}(0.25,0.25,0.50)$ along the *X*-*R* symmetry direction. However, the electron-phonon coupling parameter is found to be maximum with the value of 1.27 at this $\mathbf{q}$ point. This result clearly indicates that the largest contribution to electron-phonon interactions comes from the *X*-*R* symmetry direction. The reason of this large contribution is the large atomic displacement patterns of Ni atoms. As a result of large vibrations of Ni atoms, their *d* electrons interact with each other strongly which leads the softening of this phonon branch. It should be noted that this phonon branch also includes large atomic vibrations from Cd atoms. In order to get a more quantitative picture of electron-phonon coupling, we have calculated the Eliashberg spectral function $\alpha^2F(\omega)$ which is compared with the phonon density of states in Fig. 3. As can be seen from this figure, we find a rather good agreement between the two curves. The electron-phonon mass enhancement parameter λ and the logarithmically averaged frequency $\omega_{\ln}$ are then obtained as[37,38]

$$\lambda = \sum_{\mathbf{q}j} \lambda_{\mathbf{q}j}, \tag{4}$$

$$\omega_{\ln} = \exp\left(\frac{1}{\lambda}\sum_{\mathbf{q}j} \lambda_{\mathbf{q}j} \ln \omega_{\mathbf{q}j}\right). \tag{5}$$

The computed value of the electron-phonon mass enhancement parameter is 0.80, which is somewhat lower than the estimated value of 0.99 in Sec. III B. The logarithmically averaged frequency $\omega_{\ln}$ is found to be 89.41 K. The superconducting transition temperature T_C was estimated on the basis of the Allen-Dynes[38] modification of the McMillan formula,[39]

$$T_C = \frac{\omega_{\ln}}{1.2}\exp\left(-\frac{1.04(1+\lambda)}{\lambda-\mu^*(1+0.62\lambda)}\right), \tag{6}$$

where μ^* is a Coulomb pseudopotential. Using the above equations and taking typical values of $\mu^*=0.12$, 0.13, 0.14, and 0.15, we obtain $T_C=3.54$, 3.28,3.03, and 2.79 K, respectively. These values are in agreement with the experimental value of around 3 K.[23] Thus, our calculations indicate that $CdCNi_3$ is a BCS superconductor, in agreement with the experimental observation.[23]

Now we make a comparison of the effective superconductivity between $CdCNi_3$ and $MgCNi_3$ by analyzing their electronic and phonon structures. For BCS type superconductors, T_C depends on three factors: $N(E_F)$, λ, and $\omega_{\ln}$. The first of these has similar values for the two materials: The calculated value of $N(E_F)=3.82$ states/eV for $CdCNi_3$ is very close to the corresponding value of around 3.75 states/eV for $MgCNi_3$.[40] However, our calculated $\lambda=0.80$ for $CdCNi_3$ is nearly half that of the corresponding value of 1.5 for $MgCNi_3$. This clearly suggests that the electron-phonon interaction is relatively weaker in $CdCNi_3$. To explain this we note that there are significant differences between their phonon-dispersion curves. For $MgCNi_3$ anomalous phonon-dispersion curves have been noted along several symmetry directions (Γ-*M*, Γ-*R*, and *X*-*R*). In addition, one of the branches becomes unstable along *X*-*R*. In contrast, for $CdCNi_3$ we have only noted anomalous phonon dispersion along the *X*-*R* symmetry direction. It is well known that anomalous phonon behavior makes a large contribution to λ. In order to show this we have presented the phonon linewidth $\gamma_{\mathbf{q}j}$ for the lowest acoustic-phonon mode in Fig. 4. As can be seen from this figure, the phonon linewidth reaches a peak at 15.5 GHz along the *X*-*R* direction, for which anomalous phonon dispersion has been found. The third factor, viz., the logarithmic frequency $\omega_{\ln}$, has a lower value of 89 K for $CdCNi_3$ than 143 K (Ref. 9) for $MgCNi_3$. Thus the third factor also contributes to the lowering of T_C for $CdCNi_3$.

IV. SUMMARY

The structural, elastic, and electronic properties for $CdCNi_3$ have been studied using the density-functional theory within the generalized gradient approximation. We have observed that the main contributions to the density of states at the Fermi level come from the Ni $3d$ states. The phonon-dispersion curves do not show unstable mode, confirming that this material is dynamically stable. However, a softening behavior of the lowest acoustic branch has been predicted along the *X*-*R* symmetry direction. We have presented a numerically accurate correlation between phonon anomalies and the superconducting transition temperature (T_c) by studying electron-phonon interaction in this material. Our electron-phonon interaction results show that the phonon linewidth of the lowest acoustic-phonon mode reaches a peak value of 15.5 GHz along the *X*-*R* direction, for which anomalous phonon dispersion has been found. This result indicates that the anomalous phonon behavior is favorable to superconductivity. With a reasonable choice of 0.14 for the Coulomb pseudopotential μ^*, our estimate of the superconducting T_C of 3.03 K compares very well with the experimental value of 3.0 K.

ACKNOWLEDGMENTS

Some of the calculations for this project were carried out using the computing facilities in the School of Physics, University of Exeter, United Kingdom.

[1] T. He, Q. Huang, A. P. Ramirez, Y. Wang, K. A. Regan, N. Rogado, M. A. Hayward, M. K. Haas, J. S. Slusky, K. Inumaru, H. W. Zandbergen, N. P. Ong, and R. J. Cava, Nature (London) **411**, 54 (2001).
[2] H. Rosner, R. Weht, M. D. Johannes, W. E. Pickett, and E. Tosatti, Phys. Rev. Lett. **88**, 027001 (2001).
[3] S. Y. Li, R. Fan, X. H. Chen, C. H. Wang, W. Q. Mo, K. Q. Ruan, Y. M. Xiong, X. G. Luo, H. T. Zhang, L. Li, Z. Sun, and L. Z. Cao, Phys. Rev. B **64**, 132505 (2001).
[4] J. H. Shim, S. K. Kwon, and B. I. Min, Phys. Rev. B **64**, 180510(R) (2001).
[5] J.-Y. Lin, P. L. Ho, H. L. Huang, P. H. Lin, Y.-L. Zhang, R.-C. Yu, C.-Q. Jin, and H. D. Yang, Phys. Rev. B **67**, 052501 (2003).
[6] Z. Q. Mao, M. M. Rosario, K. D. Nelson, K. Wu, I. G. Deac, P. Schiffer, Y. Liu, T. He, K. A. Regan, and R. J. Cava, Phys. Rev. B **67**, 094502 (2003).
[7] A. Szajek, J. Phys.: Condens. Matter **13**, L595 (2001).
[8] S. B. Dugdale and T. Jarlborg, Phys. Rev. B **64**, 100508(R) (2001).
[9] A. Walte, G. Fuchs, K. H. Müller, A. Handstein, K. Nenkov, V. N. Narozhnyi, S. L. Drechsler, S. Shulga, L. Schultz, and H. Rosner, Phys. Rev. B **70**, 174503 (2004).
[10] D. J. Singh and I. I. Mazin, Phys. Rev. B **64**, 140507(R) (2001).
[11] I. Hase, Phys. Rev. B **70**, 033105 (2004).
[12] M. D. Johannes and W. E. Pickett, Phys. Rev. B **70**, 060507(R) (2004).
[13] H. M. Tütüncü and G. P. Srivastava, J. Phys.: Condens. Matter **18**, 11089 (2006).
[14] A. Y. Ignatov, S. Y. Savrasov, and T. A. Tyson, Phys. Rev. B **68**, 220504(R) (2003).
[15] R. Heid, B. Renker, H. Schober, P. Adelmann, D. Ernst, and K.-P. Bohnen, Phys. Rev. B **69**, 092511 (2004).
[16] M.-S. Park, J. Giim, S.-H. Park, Y. W. Lee, S. I. Lee, and E. J. Choi, Supercond. Sci. Technol. **17**, 274 (2004).
[17] C. M. I. Okoye, Solid State Commun. **136**, 605 (2005).
[18] P. Tong, Y. P. Sun, X. B. Zhu, and W. H. Song, Phys. Rev. B **73**, 245106 (2006).
[19] P. Tong, Y. P. Sun, X. B. Zhu, and W. H. Song, Phys. Rev. B **74**, 224416 (2006).
[20] P. J. T. Joseph and P. P. Sigh, J. Phys.: Condens. Matter **18**, 5333 (2006).
[21] M. Sieberer, P. Mohn, and J. Redinger, Phys. Rev. B **75**, 024431 (2007).
[22] M. Uehara, T. Amano, S. Takano, T. Kori, T. Yamazaki, and Y. Kimishima, Physica C **440**, 6 (2006).
[23] M. Uehara, T. Yamazaki, T. Kori, T. Kashida, Y. Kimishima, and I. Hase, J. Phys. Soc. Jpn. **76**, 034714 (2007).
[24] I. R. Shein and A. L. Ivanovskii, Phys. Rev. B **77**, 104101 (2008).
[25] I. R. Shein, V. V. Bannikov, and A. L. Ivanovskii, Physica C **468**, 1 (2008).
[26] D. Vanderbilt, Phys. Rev. B **41**, 7892 (1990).
[27] J. P. Perdew, K. Burke, and M. Ernzerhof, Phys. Rev. Lett. **77**, 3865 (1996).
[28] H. J. Monkhorst and J. D. Pack, Phys. Rev. B **13**, 5188 (1976).
[29] M. J. Mehl, J. E. Osburn, D. A. Papaconstantopoulos, and B. M. Klein, Phys. Rev. B **41**, 10311 (1990).
[30] P. Söderlind, O. Eriksson, J. M. Wills, and A. M. Boring, Phys. Rev. B **48**, 5844 (1993).
[31] S. Baroni, P. Giannozzi, and A. Testa, Phys. Rev. Lett. **58**, 1861 (1987).
[32] S. Baroni, S. de Gironcoli, A. Dal Corso, and P. Giannozzi, Rev. Mod. Phys. **73**, 515 (2001); http://www.pwscf.org
[33] D. A. Papaconstantopoulos and W. E. Pickett, Phys. Rev. B **45**, 4008 (1992).
[34] F. D. Murnaghan, Proc. Natl. Acad. Sci. U.S.A. **50**, 697 (1944).
[35] M. Born and K. Huang, *Dynamical Theory of Crystal Lattices* (Clarendon, Oxford, 1956).
[36] W. Weber, Phys. Rev. B **8**, 5093 (1973).
[37] P. B. Allen, Phys. Rev. B **6**, 2577 (1972).
[38] P. B. Allen and R. C. Dynes, Phys. Rev. B **12**, 905 (1975).
[39] W. L. McMillan, Phys. Rev. **167**, 331 (1968).
[40] H. M. Tütüncü and G. P. Srivastava (unpublished).